

# Force and virial formula in the linear combination of atomic orbitals $X\alpha$ method and its application to oxygen chemisorption on the Al(111) and Mg(0001) surfaces

Chikatoshi Satoko

*Institute for Molecular Science, Myodaiji, Okazaki, Aichi 444, Japan*

(Received 14 November 1983; revised manuscript received 6 February 1984)

An expression for the gradient (with respect to nuclear coordinates) of the electronic total energy is given using the LCAO- $X\alpha$  method and related to the virial. The formulas are extended to the linear combination of plane waves (LCPW) method. Our method is applied to the chemisorption of oxygen on Al(111) and Mg(0001) surfaces. The calculations are performed using O/Al<sub>4</sub> and O/Mg<sub>4</sub> model clusters with the metal-metal distance equal to the bulk. The calculated forces explain the experiments which report that oxygen is not absorbed below the Al surface but is absorbed below the Mg surface. The difference in the chemisorption processes is due to differences in the strength of the metal-metal bond interaction.

## I. INTRODUCTION

The calculation of the atomic forces and the surface pressure is useful in estimating equilibrium positions, bulk moduli, elastic constants, and the degree of lattice vibration of molecules and solids. The atomic forces and the surface pressure have been derived from both the Hellmann-Feynman theorem and the virial theorem.<sup>1-3</sup> These theorems are, however, valid only for rigorous eigenfunctions of the Hamiltonian.<sup>4</sup> It is very difficult to obtain rigorous eigenfunctions for self-consistent Hartree-Fock-Slater  $X\alpha$  (HFS  $X\alpha$ ) equations. Several approximations have been proposed to overcome this. For an example, one can replace the real potential by a spherically symmetric potential such as the muffin tin. The use of this approximation has led to the development of many methods, such as the scattered-wave  $X\alpha$  (SW  $X\alpha$ ) method, the augmented-plane-wave (APW) method, and the Korringa-Kohn-Rostoker (KKR) method.<sup>5,6</sup> However, the spherically symmetric approximation is not useful for molecules and surfaces.

Another approximation is to limit the variational parameters in the coefficients of the linear combination of atomic orbitals<sup>7</sup> or plane waves.<sup>8-10</sup> In any case, for the calculation of the atomic forces and the surface pressure using approximate wave functions, one should take into account corrections to the Hellmann-Feynman and virial theorems. These corrections have been ignored in almost all calculations performed so far. To circumvent the limitations of the Hellmann-Feynman force calculation, the force was calculated by an approximation: the valence-only energy-functional method.<sup>11</sup> Correction terms are required even in this case.

In this paper we derive the correction terms to the Hellmann-Feynman theorem and the virial theorem. These theorems (with correction terms) are applied to the cases of oxygen chemisorption on Al(111) and Mg(0001) surfaces.

## II. DERIVATIVES OF THE TOTAL ENERGY

The calculation of the derivative of the total energy with respect to the atom coordinate in the *ab initio* SCF

theory has been discussed previously.<sup>12,13</sup> Here we provide a general formula for the derivative of the total energy with respect to any parameter representing the atomic coordinate, the scaling of wave functions, or an external field such as a magnetic field or an electric field.

The total energy  $E$  in the  $X\alpha$  theory<sup>1</sup> is given by

$$E = \frac{1}{2} \sum_{\mu, \nu} \frac{Z_{\mu} Z_{\nu}}{R_{\mu\nu}} - \sum_{\nu} Z_{\nu} \int \frac{\rho(\vec{r})}{r_{\nu}} dv + \frac{1}{2} \int \int \rho(\vec{r}) \frac{\rho(\vec{r}')}{|\vec{r} - \vec{r}'|} dv dv' + E_{\text{kin}} + E_{\text{xc}}, \quad (1)$$

where  $E_{\text{kin}}$  and  $E_{\text{xc}}$  are the kinetic and the  $X\alpha$  exchange-correlation energy written as follows:

$$E_{\text{kin}} = \sum_i^{\text{occ}} \int \phi_i^* \left( -\frac{1}{2} \vec{\nabla}^2 \right) \phi_i dv \quad (2)$$

and

$$E_{\text{xc}} = \frac{-9\alpha}{8} \left[ \frac{3}{\pi} \right]^{1/3} \int \rho(\vec{r})^{4/3} dv. \quad (3)$$

The first, second, and third terms on the right-hand side of Eq. (1) are the nuclear-nuclear repulsion, and the electron-nuclear and electron-electron electrostatic interactions, respectively. The nuclear charge  $Z_{\mu}$  is for the  $\mu$ th atom,  $\rho(\vec{r})$  is the electron density, and  $\vec{R}_{\mu}$  is the atom coordinate. The one-electron HFS wave equation derived variationally from Eq. (1) is written as

$$\tilde{h}\phi_i = \epsilon_i \phi_i, \quad (4)$$

and

$$\tilde{h} = -\frac{\vec{\nabla}^2}{2} - \sum_{\mu} \frac{Z_{\mu}}{r_{\mu}} + \int \frac{\rho(\vec{r}')}{|\vec{r} - \vec{r}'|} dv + V_{\text{xc}}(\vec{r}), \quad (5)$$

where  $\rho(\vec{r})$  is the charge density defined by

$$\rho(\vec{r}) = \sum_i^{\text{occ}} \phi_i^* \phi_i, \quad (6)$$

and  $V_{\text{xc}}(\vec{r})$  is the Slater  $X\alpha$  potential defined by

$$V_{xc}(\vec{r}) = -\frac{3\alpha}{2} \left[ \frac{3\rho(\vec{r})}{\pi} \right]^{1/3}. \quad (7)$$

The molecular orbital  $\phi_i$  is obtained from the solution of the  $X\alpha$  equation (4). However, it is so difficult to solve the  $X\alpha$  equation for molecules and solids that the following approximation is adopted. The molecular orbital is approximated by the linear combination of basis sets, such as atomic orbitals (LCAO) or plane waves (LCPW). The coefficients are variationally determined by the minimization of the total energy. If the number of the basis sets are infinite and comprise a complete set, the molecular orbitals obtained are exact solutions of Eq. (4). However, the calculation using the infinite basis set is clearly impossible.

We now derive the derivative of the total energy with respect to an arbitrary parameter  $\lambda$  for  $\lambda = \lambda_0$ . The total energy of Eq. (1) is a function of the basis sets, the coefficients of the basis sets, and the parameter  $\lambda$ , which may be the atomic coordinate, the scaling factor, or the external field. The Hamiltonian, the basis sets, and the coefficients depend, in general, on the parameter. Let the molecular orbital be defined as the linear combination of the basis

$$\psi_i(\lambda) = \sum_j u_j(\lambda) C_j^i(\lambda), \quad (8)$$

where the basis  $u_j$  is given by a linear combination of atomic orbitals or plane waves, but the coefficients of the combination are fixed only at  $\lambda = \lambda_0$ . The coefficients  $C_j^i$  of the linear combination are determined by minimizing the following equation:

$$\Delta = E(\{u\}, \{C\}, \lambda) - \sum_i \epsilon_i [(\psi_i, \psi_i) - 1], \quad (9)$$

where the first term is the total energy and the second term comes from the normalization condition of the molecular orbital; the  $\epsilon_i$ 's are Lagrange's undetermined multipliers. The result is the well-known secular equation

$$\left[ \frac{\partial E}{\partial C_j^i} \right]_{\lambda, \mu} = 2\epsilon_i \sum_k S_{jk} C_i^k, \quad (10)$$

where the  $S_{jk}$  are overlap matrices between the  $j$ th and  $k$ th molecular orbitals. The secular equation is also written as

$$\sum_k (u_j, h u_k) C_i^k = \epsilon_i \sum_k S_{jk} C_i^k. \quad (11)$$

The one-electron Hamiltonian  $h$  is similar to that in Eq. (5), but differs from it in that the electron density  $\rho(\vec{r})$  is not defined by Eq. (6) but rather by the following equation:

$$\rho(\vec{r}) = \sum_i^{\text{occ}} \psi_i^* \psi_i. \quad (12)$$

This secular equation (11) means the wave function  $\psi_i$  is not the solution of Eq. (4), but is the solution of the following equation:

$$h\psi_i = \epsilon_i \psi_i + w_i, \quad (13)$$

where  $w_i$  is a certain function orthogonal to the wave function  $\psi_i$ ,

$$(\psi_i, w_j) = 0 \text{ for any } i \text{ and } j. \quad (14)$$

The function  $w_i$  is not generally zero and depends on the incompleteness of the basis set.

Here we choose the coefficients of atomic orbitals in the basis  $u_j$  as the solution  $\psi_j$  of the secular equation (11) at the value of  $\lambda = \lambda_0$ , i.e.,

$$C_i^j(\lambda_0) = \delta_{ij}. \quad (15)$$

This definition simplifies the following derivation and does not lose generality. The basis function  $u_j(\lambda)$  is not the eigenfunction of the HFS equation except at  $\lambda = \lambda_0$ .

Now, by using Eq. (10), the derivative of the total energy with respect to any parameter  $\lambda$  is written as

$$\begin{aligned} \frac{dE(\{u\}, \{C\}, \lambda)}{d\lambda} &= \left[ \frac{\partial E}{\partial \lambda} \right]_{u, C} + \sum_j \left[ \frac{\delta E}{\delta u_j} \right]_{\lambda, C} \frac{du_j}{d\lambda} \\ &\quad + \sum_i^{\text{occ}} 2\epsilon_i \sum_{j, k} S_{jk} \frac{dC_j^i}{d\lambda} C_i^k. \end{aligned} \quad (16)$$

The last term is simplified at  $\lambda = \lambda_0$  by using Eq. (15) and the condition that the derivative of the norm of the molecular orbital with respect to the parameter is equal to zero,

$$2 \sum_{j, k} S_{jk} \frac{dC_j^i}{d\lambda} C_i^k = - \left[ \frac{dS_{ii}}{d\lambda} \right]_{\lambda = \lambda_0}. \quad (17)$$

The final expression of the derivative of the total energy at  $\lambda = \lambda_0$  is written as the following equation:

$$\frac{dE}{d\lambda} = \left[ \frac{\partial E}{\partial \lambda} \right]_{u, C} + \sum_i^{\text{occ}} \int \frac{\partial u_i^*}{\partial \lambda} (h - \epsilon_i) u_i dv + \text{c.c.} \quad (18)$$

The first term of Eq. (18) is the Hellmann-Feynman term and the second term is the correction for the approximate eigenfunction. The second term is vanishing if the molecular orbital is the true eigenfunction of Eq. (4).

### III. THE FORCES AND THE VIRIAL

The method of calculating the forces and the virial provides a powerful tool for theoretical studies of molecules, surface geometries, and reaction paths. In this section we derive the force and the virial formulas in the LCAO and LCPW approximations.

The force acting on the  $\mu$ th atom is given by the minus derivative of the total energy with respect to the  $\mu$ th nuclear coordinate. For the calculation using approximate eigenfunctions, one should take not only the Hellmann-Feynman force into account, but also the force arising from the derivative of the wave function. In the LCPW approximation the Hellmann-Feynman force is exact since the correction term is vanishing: The plane waves are independent of the atomic coordinates. In the LCAO approximation one can obtain the force formula acting on the  $\mu$ th atom by using Eq. (18) and  $\lambda = R_\mu$ ,

$$\vec{F}_\mu = -\frac{\partial E}{\partial \vec{R}_\mu} = \vec{F}_{\mu 1} + \vec{F}_{\mu 2}, \quad (19)$$

where  $\vec{F}_{\mu 1}$  is the Hellmann-Feynman term,

$$\vec{F}_{\mu 1} = -Z_\mu \sum_v Z_v \frac{\vec{R}_{\mu v}}{R_{\mu v}^3} + Z_\mu \int \rho(\vec{r}) \frac{\vec{r}_\mu}{r_\mu^3} dv, \quad (20)$$

and the correction term  $\vec{F}_{\mu 2}$  comes from the derivative of the wave function with respect to  $\vec{R}_\mu$ ,

$$\vec{F}_{\mu 2} = - \left[ \sum_i^{\text{occ}} \int \frac{\partial \psi_i^*}{\partial \vec{R}_\mu} (h - \epsilon_i) \psi_i dv + \text{c.c.} \right], \quad (21)$$

where  $\psi_i$  is the molecular orbital obtained from the solution of the HFS equation (13) in the LCAO approximation. Note that the derivative with respect to the nuclear coordinate  $\vec{R}_\mu$  in the second term is done by regarding the coefficients of the linear combination of the atomic orbitals as constants. Such a formula has already been published,<sup>13</sup> but we shall rewrite the main terms in the following discussion.

Each term of the force,  $\vec{F}_{\mu 1}$  and  $\vec{F}_{\mu 2}$ , depends sensitively on the basis sets of the LCAO approximation, so that, if the exact eigenfunctions are not used, each term has no physical meaning. However, if the exact eigenfunctions are used, the Hellmann-Feynman force is the electrostatic force acting on the nuclear charge due to both the surrounding electronic charges and the other nuclear charges. If the nuclear charges involved are large, the inaccuracy of the eigenfunctions brings about a large change in the Hellmann-Feynman force. Such change is cancelled by the correction  $\vec{F}_{\mu 2}$  so that the sum of the forces  $\vec{F}_{\mu 1}$  and  $\vec{F}_{\mu 2}$  is insensitive to the choice of the basis sets. Therefore we decompose the force  $\vec{F}_\mu$  into the pair forces due to a particular atom which is given in terms of  $\rho_\mu(\vec{r})$  defined as

$$\rho_\mu(\vec{r}) = \sum_i^{\text{occ}} \psi_{i\mu} \psi_i, \quad (22)$$

where  $\psi_{i\mu}$  is the atomic part of  $\psi_i$  associated with the  $\mu$ th atom as shown by

$$\psi_i(\vec{r}) = \sum_\mu \psi_{i\mu}(\vec{r} - \vec{R}_\mu). \quad (23)$$

The integrated value of  $\rho_\mu(\vec{r})$  over space corresponds to the Mulliken charge of the  $\mu$ th atom. The total electron density is written as

$$\rho(\vec{r}) = \sum_\mu \rho_\mu(\vec{r}). \quad (24)$$

The breakdown of the force into the pair force may be expressed as

$$\vec{F}_\mu = \sum_\tau \vec{f}_\mu^\tau, \quad (25)$$

where the pair force  $\vec{f}_\mu^\tau$  due to the  $\tau$ th atom is given by three terms. The first term is the electrostatic force acting on the  $\mu$ th atom due to the  $\tau$ th atom,

$$\vec{f}_{\mu 1}^\tau = Z_\mu \vec{E}_\tau(\vec{R}_\mu) - \int \rho_\mu(\vec{r}) \vec{E}_\tau(\vec{r}) dv, \quad (26)$$

where  $\vec{E}_\tau(\vec{r})$  is the electric field due to the nuclear and electronic charge of the  $\tau$ th atom,

$$\vec{E}_\tau(\vec{r}) = Z_\tau \vec{r}_\tau / r_\tau^3 - \int \frac{\rho_\tau(\vec{r}')(\vec{r} - \vec{r}')}{|\vec{r} - \vec{r}'|^3} dv'. \quad (27)$$

The second term is the force due to the derivative of the terms' wave functions with respect to the nuclear coordinate,

$$\vec{f}_{\mu 2}^\tau = \sum_i^{\text{occ}} \int \left[ \frac{\partial \psi_{i\mu}}{\partial \vec{r}} (h - \epsilon_i) \psi_{i\tau} - \frac{\partial \psi_{i\tau}}{\partial \vec{r}} (h - \epsilon_i) \psi_{i\mu} \right] dv. \quad (28)$$

The third term is due to the  $X\alpha$  exchange-correlation potential

$$\vec{f}_{\mu 3}^\tau = \frac{1}{4} \int \left[ \frac{d\rho_\mu}{d\vec{r}} \rho_\tau - \frac{d\rho_\tau}{d\vec{r}} \rho_\mu \right] V_{xc}(\vec{r}) \rho^{-1}(\vec{r}) dv. \quad (29)$$

The force  $\vec{f}_1$  is derived from the assumption that the Mulliken charge distribution does not change for the infinitesimal displacement of the nuclear coordinates. The force  $\vec{f}_2$  for ionic materials is long ranged. The force  $\vec{f}_2$  is due to the change of the Mulliken charge population, i.e., charge transfer, charge polarization, and charge relaxation. The force  $\vec{f}_3$  is due to the field defined as the minus gradient of the  $X\alpha$  potential. A proof of Eqs. (26), (28), and (29) is given in Appendix A.

Slater has shown that the virial is given as [Eqs. (A2-6)–(A2-15) of Slater's book<sup>14</sup>]:

$$\sum_\mu \vec{R}_\mu \cdot \frac{dE}{d\vec{R}_\mu} = -2E_{\text{kin}} - V - \left[ \frac{dE}{d\lambda} \right]_{\lambda=1}. \quad (30)$$

where  $\lambda$  is the scaling parameter of the wave functions defined as

$$\psi_i(\lambda) = \lambda^{-3/2} W_i(\vec{r}/\lambda, \vec{R}_1/\lambda, \vec{R}_2/\lambda, \dots). \quad (31)$$

If the total energy is minimized with respect to the scaling parameters, we have

$$\left[ \frac{dE}{d\lambda} \right]_{\lambda=1} = 0. \quad (32)$$

However, the total energy in the LCAO or LCPW approximations is not always minimized with respect to the scaling parameter. The derivative of the wave function with respect to the scaling is given as

$$\left[ \frac{\partial \psi_i}{\partial \lambda} \right]_{\lambda=1} = -\vec{r} \cdot \frac{\partial \psi_i}{\partial \vec{r}} - \sum_\mu \vec{R}_\mu \cdot \frac{\partial \psi_i}{\partial \vec{R}_\mu} - \frac{3}{2} \psi_i. \quad (33)$$

By using Eqs. (18), (30), and (33), one obtains

$$\sum_{\mu} \vec{R}_{\mu} \cdot \vec{F}_{\mu} = 2E_{\text{kin}} + \bar{V} - \sum_{\mu} \sum_i^{\text{occ}} \int \left( (\vec{r} - \vec{R}_{\mu}) \cdot \frac{\partial \psi_{i\mu}^*}{\partial \vec{r}} (h - \epsilon_i) \psi_i + \text{c.c.} \right) dv, \quad (34)$$

for the LCAO approximation, and

$$\sum_{\mu} \vec{R}_{\mu} \cdot \vec{F}_{\mu} = 2E_{\text{kin}} + \bar{V} - \sum_i^{\text{occ}} \int \left[ \vec{r} \cdot \frac{\partial \psi_i^*}{\partial \vec{r}} (h - \epsilon_i) \psi_i + \text{c.c.} \right] dv, \quad (35)$$

for the LCPW approximation. These formulas can also be derived from the force formulas in Eqs. (19)–(21), as proved in Appendix B.

We have written a program to calculate the force in the LCAO  $X\alpha$  theory. The pair forces are calculated using the self-consistent wave functions of the HFS equation (11). The HFS and force matrix elements are numerically evaluated with the use of the following method. The integration space is divided into the Wigner-Seitz cells around each atom. The integration within each cell is done by the Gaussian quadrature method and the angular quadrature method when the integration is in the radial direction and the angular direction, respectively.<sup>15</sup> The Coulomb potential in the self-consistent cycle is evaluated by the summation of the multipole potential. The multipole of each atom is determined by least-squares fitting to the charge distribution. The least-squares deviation is defined as the following equation:

$$\Delta_L = \int \left[ \rho(\vec{r}) - \sum_i n_i \rho_i(\vec{r}) \right]^2 w(\vec{r}) dv, \quad (36)$$

where  $w(\vec{r})$  is the weight function

$$w(\vec{r}) = \sum_{\mu} \frac{1}{|\vec{r} - \vec{R}_{\mu}|^2}. \quad (37)$$

This weight function is chosen so that the better the charge distribution is fitted, the better the multipole potential is fitted to the true Coulomb potential. The basis set for the charge fitting is the spherical harmonics multiplied by the square of the atomic radial orbitals,

$$\rho_{i=nlm}(\vec{r}) = R_{nl}^2(\vec{r}) Y_{lm}(\theta, \varphi). \quad (38)$$

In the next section we shall apply these force and virial analyses to the study of the equilibrium geometry of a chemisorbed oxygen atom on the Al(111) and Mg(0001) surfaces.

#### IV. APPLICATIONS OF THE FORCE AND VIRIAL ANALYSES

Oxidation processes on metal surfaces have been studied by many experimental methods such as low-energy electron diffraction (LEED), x-ray photoelectron spectroscopy (XPS), Auger-electron spectroscopy (AES), energy-loss spectroscopy (ELS), and surface-extended x-ray-absorption fine-structure spectroscopy (SEXAFS). Oxygen molecules are chemisorbed as molecules or dissociated atoms depending upon the oxygen pressure and the substrate temperature.<sup>16</sup> The dissociated atoms form a superlattice structure on the surface or incorporate into the surface. The chemisorption of  $O_2$  on the Al and Mg surfaces

causes the emission of photons or electrons<sup>17,18</sup> at much lower pressures of  $O_2$ . Dissociated oxygen atoms on the Al(111) surface are chemisorbed at the threefold centered hollow site,<sup>19</sup> while oxygen atoms on Mg(0001) are absorbed in the surface lattice plane.<sup>20</sup> The distortion of the surface lattice also occurs when a chemisorbed atom approaches the surface to be chemisorbed. It is important to consider such a distortion in the chemisorption process.<sup>21</sup> The activation energy of the chemisorbed atom may sensitively depend on the surface distortion. The analysis of the force calculation is very important in deciding whether the surface atoms are pulled outwards or pressed inwards by the chemisorbed atom, while the analysis of the total-energy calculation is not. To understand these chemisorption processes, we calculate the force and the virial as functions of the distance of the oxygen atom from the surface plane.

##### A. Force and virial analyses of diatomic molecules AlO

We have studied the AlO bond distance using force analysis with the numerical basis of the neutral Al( $1s^2 2s^2 2p^6 3s^2 3p$ ) and O( $1s^2 2s^2 2p^4$ ). Figure 1 shows the change of the calculated pair force  $f$  between Al and O as a function of the distance  $D$  between Al and O. We obtained the equilibrium bond distance 3.07 a.u. This value agrees fairly well with the experimental value of 3.05 a.u.<sup>22</sup> This force is decomposed into the electrostatic force  $f_1$  of Eq. (26), the deformed-charge force  $f_2$  of Eq.

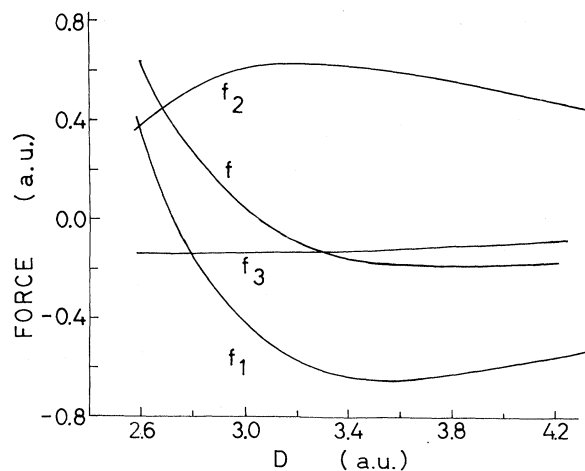


FIG. 1. Calculated pair force  $f$  and its components  $f_1$ ,  $f_2$ , and  $f_3$  for the molecule AlO as functions of the distance between Al and O. Positive force means repulsion between Al and O. (In all figures, a.u. denotes atomic units.)

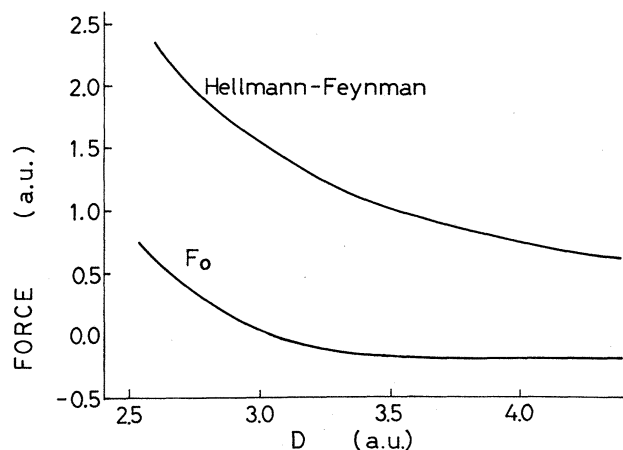


FIG. 2. Calculated Hellmann-Feynman and corrected total forces acting on the oxygen atom in the molecule AlO.

(28), and the exchange force of Eq. (29), as shown in Fig. 1. The electrostatic force  $f_1$  sensitively depends upon the distance  $D$  changing sign at 2.73 a.u. The deformed-charge force  $f_2$  and the exchange force  $f_3$  are rather insensitive to change in  $D$ . The former is always repulsive and the latter attractive. The force  $f$  consisting of the sum of the three forces is almost cancelled at  $D$  near and beyond the equilibrium bond distance and is comparable with the exchange force  $f_3$ .<sup>23</sup>

We have studied the order of magnitude of the correction term in the force formula (19) and the virial formula (34). The calculated Hellmann-Feynman force  $\vec{F}_{O(1)}$  and corrected total force  $\vec{F}_O$  of the molecule AlO are shown in Fig. 2 as functions of the bond distance  $D$ . The force  $\vec{F}_{O(1)}$  is very much different from the corrected force  $F_O$ . A large part of this difference comes from an insufficient core polarization in the LCAO approximation.<sup>11</sup> The bonding properties cannot be discussed without consideration of the correction term of Eq. (19). The order of magnitude of the Hellmann-Feynman force is very much dependent on the basis set used in the LCAO approximation. Figure 3 shows the first two terms,  $2E_{\text{kin}} + V$ , of Eq.

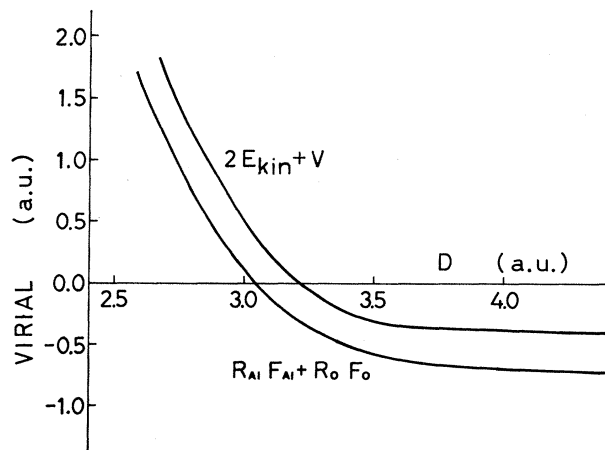


FIG. 3. Calculated  $2E_{\text{kin}} + V$  and virial of the molecule AlO.

(34), and the virial of the molecule AlO as a function of  $D$ . The difference between the two curves is due to the correction term in the virial formula (34). This is not as large as the correction term in the force formula (19). The force is not averaged over the region surrounding the atoms, but the virial is.<sup>1</sup>

#### B. Chemisorption of an oxygen atom on Al-metal surface

For this system, a brief report on the calculated forces acting on the atoms and the potential curve at the Al(111) surface has already been published.<sup>13</sup> We first mention the model cluster for this system. This is composed of an oxygen atom, the triangle Al(1)<sub>3</sub> cluster, and an Al(2) atom below the center of the triangle, as shown in Fig. 4. The oxygen atom is chemisorbed at the threefold centered hollow sites above the triangle. We calculate the electronic structure and the force as a function of the height of the oxygen atom above or below the center of the Al(1)<sub>3</sub>. The bond distances between Al—Al metals are fixed at the bond distance of the bulk.<sup>24,25</sup>

The electronic structure is shown in Fig. 5 as a function of the height of the oxygen. The main components of each state are indicated on the right-hand side of each line. The states  $1a_1$  and  $1e$  are mainly composed of the O  $2p$  orbitals perpendicular to the surface. The  $2a_1$ ,  $3a_1$ , and  $2e$  states are mainly composed of Al  $3s$ -orbitals. The states whose energies are above  $-0.1$  a.u. mainly come from Al  $3p$  orbitals. The highest occupied level,  $3e$ , belongs to the state in which the Al  $3p$  orbitals are antibondingly coupled with the O  $2p$  orbitals. In the  $2a_1$ ,  $3a_1$ , and  $2e$  states the Al  $3s$  orbital is bondingly coupled with the oxygen  $2p$  orbitals. The photoemission spectra of the oxygen adsorbed on the clean Al surface show an asymmetric broadband due to the oxygen  $2p$  electrons about 7.2 eV below the Fermi energy.<sup>26,27</sup> Our calculated levels of the oxygen  $2p$  orbital are located at 6.7 and 7.4 eV below the Fermi energy, which are excited by photons polarized perpendicular and parallel to the surface, respectively. The broadening may be due to the splitting of the oxygen  $2p$  orbitals.

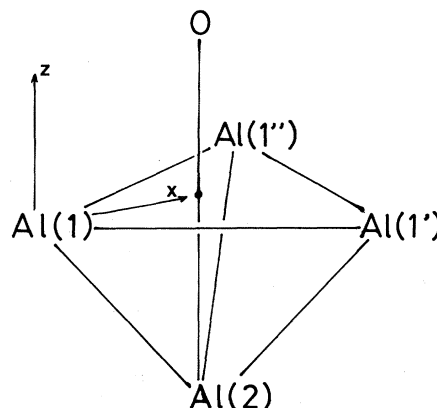


FIG. 4. Geometry of the model cluster O/Al(1)<sub>3</sub>Al(2).

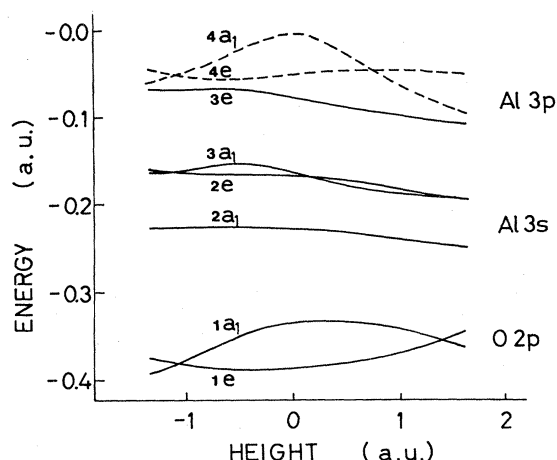


FIG. 5. Calculated electronic structure of the  $O/Al_4$  cluster as a function of oxygen height. The levels are classified into three groups composed mainly of the  $O\ 2p$ ,  $Al\ 3s$ , and  $Al\ 3p$  orbitals, respectively. The dashed lines signify unoccupied orbitals.

The solid curves of Fig. 6 represent the pair forces between the atoms of the  $Al(1)_3OAl(2)$  cluster calculated from Eqs. (26), (28), and (29) of the preceding subsection. The dashed curves are the corresponding pair forces in the  $AlO$  molecule. The pair force in the cluster is not directed along the bond between the atoms since this pair force includes the influence of atoms effectively outside the pair. The pair force in Fig. 6 is the component parallel to the bond direction. The positive (negative) pair force is defined as repulsive (attractive). The force perpendicular to the bond direction is small and can be neglected in the present case.

The pair force  $f_{O}^{Al(1)}$  between the oxygen and the surface  $Al(1)$  is always negative, i.e., attractive for any height  $R_h$  of the oxygen above the surface, as shown by solid curves in Fig. 6. The height dependence of this force is similar to that of the interaction  $f_{O}^{Al(1)}(AlO)$  in the  $AlO$

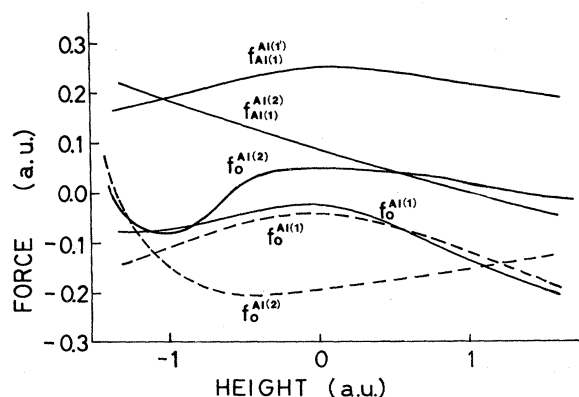


FIG. 6. Effective pair forces among the  $O$ , the first-layer  $Al(1)$ , and the second-layer  $Al(2)$  atoms as functions of oxygen height. The positive force is defined to be in the direction of the pair bond, i.e., repulsive. Positive (negative) height corresponds to the position above (below) the surface. The dashed lines show the corresponding pair forces of the  $AlO$  molecule.

molecule, as shown by dashed curves in Fig. 6. On the other hand, the pair force  $f_{O}^{Al(2)}$  between the oxygen and the second-layer atom  $Al(2)$  is repulsive when the oxygen atom is located near the surface ( $R_h \approx 0$ ), and attractive when it is located more than 0.6 a.u. below the surface ( $z \approx -0.6$ ), and finally  $f_{O}^{Al(2)}$  becomes repulsive again when the oxygen approaches the  $Al(2)$  ( $R_h \approx -1.0$ ). This dependence of the pair force  $f_{O}^{Al(2)}$  on height is very different from that of the pair force  $f_{O}^{Al(2)}(AlO)$  of the  $AlO$  molecule, which is indicated by the dashed curves in Fig. 6.

The pair force  $f_{Al(1)'}^{Al(1)}$  between the first-layer atoms  $Al(1)$  and  $Al(1')$  does not change, as this interaction is not under the influence of the bonding with the oxygen atom. On the other hand, the pair force  $f_{Al(1)}^{Al(2)}$  between the  $Al(1)$  and the  $Al(2)$  atoms becomes more repulsive as the oxygen atom moves into the surface ( $R_h \leq 0$ ).

The calculated virials, i.e., the summation of the scalar products between the nuclear coordinate and the force, are shown in Fig. 7 as a function of oxygen height. The virial of the cluster means the stress<sup>14</sup> which is necessary to maintain the cluster shape as it is given. The stress is found to increase when the oxygen approaches the surface from the outside. The stress is maximum when the oxygen is slightly below the surface. The stress decreases when the oxygen penetrates further into the surface, and begins to increase again when the oxygen approaches the second-layer  $Al(2)$ .

The equilibrium position of the oxygen atom above the  $Al$  surface is at the point where the attractive force  $f_{O}^{Al(1)}$  and the repulsive force  $f_{O}^{Al(2)}$  are balanced. The force acting on the oxygen atom is zero at  $R_h = 1.0$  a.u., as shown in Fig. 1 in a previous paper.<sup>13</sup> This position is in good agreement with both the experimental results of XPS (Refs. 28 and 29) and EXAFS (Ref. 30), but is different from the value of 2.51 a.u. derived from LEED analysis.<sup>31</sup> The LEED value at low oxygen pressures seems to correspond to the position of the undissociated molecular oxygen.<sup>17</sup>

The activation energy for penetration of oxygen into the surface comes from the repulsive force due to the second-layer  $Al(2)$ , and not from the attractive force due to the first-layer  $Al(1)$ . When the oxygen approaches the sur-

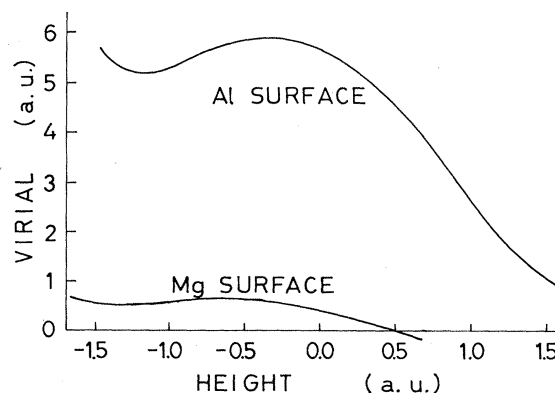


FIG. 7. Virial of the  $O/Al_4$  and  $O/Mg_4$  clusters as a function of oxygen height.

face, the oxygen bonds with the surface atom. At the same time, the bonds between the surface atoms are broken. The dependence of the attractive force  $f_{\text{O}}^{\text{Al}(1)}$  on the height  $R_h$  of the oxygen is similar to that of the AlO molecule. The force  $f_{\text{O}}^{\text{Al}(1)}$  is due to the direct bond making between the O atom and the Al(1) atom. The behavior of the repulsive force  $f_{\text{O}}^{\text{Al}(2)}$  is much different from the force between the atoms of the AlO molecule, as shown in Fig. 6. The force is not given by the simple two-body interaction between the O and Al(2) atoms, but instead by the many-body interaction between the O, Al(1), and Al(2) atoms. The repulsion of the force  $f_{\text{O}}^{\text{Al}(2)}$  is due to the bond breaking between surface atoms. Both bond making and bond breaking always occurs in the chemisorption and absorption reaction. Generally, there are three possibilities according to the sizes of the forces. Firstly, when the force for the bond making is weak, then the surface does not chemisorb atoms. Secondly, when the force for bond making exceeds the force for bond breaking, then the atom is chemisorbed on the surface. Thirdly, when the force for bond breaking is weak, then the atom is chemisorbed under the surface. The case of chemisorption on the Al surface is the second.

### C. Chemisorption of oxygen on a Mg-metal surface

We have calculated the electronic structure and the forces acting on atoms on the Mg(0001) surface. The tetragonal  $\text{Mg}_4$  cluster was chosen as the model for the Mg(0001) surface. The Mg—Mg bond distance was taken as the unrelaxed value, 6.06 a.u., of the solid.<sup>32</sup>

The change of the position of the energy levels is shown in Fig. 8 as a function of the oxygen height. The main component of each level is indicated on the right-hand side of each line. The dependence of the positions of the energy levels on oxygen height is similar to that of the O/Al<sub>4</sub> cluster. It is different from the O/Al<sub>4</sub> cluster in that the 3e level is unoccupied in the O/Mg<sub>4</sub> cluster. The

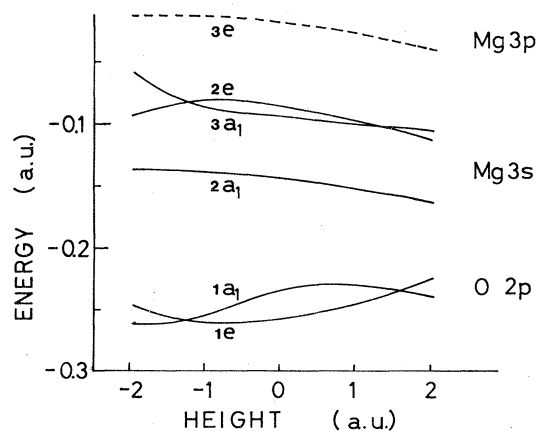


FIG. 8. Electronic structure of the O/Mg<sub>4</sub> cluster as a function of the oxygen height. The main component of each level is written on the right-hand side of the lines. The level signified by the dashed line is unoccupied.

calculated energy separation between the 1a<sub>1</sub> level and the Fermi level near the 3a<sub>1</sub> level is about 4.8 eV for  $R_h = -1.3$  a.u. (oxygen height). Photoemission spectra for oxygen adsorbed on Mg show the peak due to the O 2p electrons to be at 6.0 eV below the Fermi energy.<sup>33</sup> Therefore, the agreement is fair.

The forces acting on the oxygen, the first-layer Mg(1), and the second-layer Mg(2) are shown in Fig. 9 as a function of oxygen height. The force acting on oxygen above the surface is always toward the surface. Oxygen is absorbed below the surface without an activation energy. The position at which the force acting on oxygen is vanishing is found to be 1.3 a.u. The force acting on the first-layer Mg(1) is always very small irrespective of the position of the oxygen. The force acting on the second-layer Mg(2) changes from pushing down to pulling up toward the surface at the oxygen height of  $-1.0$  a.u.

The pair interactions are shown in Fig. 10 as a function of oxygen height. The interaction of oxygen with the first-layer Mg(1) atom and the second-layer Mg(2) atom in the cluster is found to be similar to the interaction of oxygen with Mg in the MgO molecule. The pair interactions of the first-layer Mg(1) with the other first-layer Mg(1') and with the second-layer Mg(2) atoms behaves similarly to those of the Al(1) atoms on Fig. 6. However, the repulsive interaction  $f_{\text{Mg}(1)}^{\text{Mg}(2)}$  between the Mg(1) and the Mg(2) atoms is weaker than that between the Al(1) and the Al(2) atoms.

The virial of the O/Mg<sub>4</sub> cluster is shown in Fig. 7 as a function of oxygen height. The virial of the O/Mg<sub>4</sub> is found to be smaller than that of the O/Al<sub>4</sub> cluster. The virial does not change much with oxygen absorption. There is no activation energy for oxygen adsorption on the Mg(0001) surface since the interaction between oxygen and the second-layer Mg(2) atom is attractive.

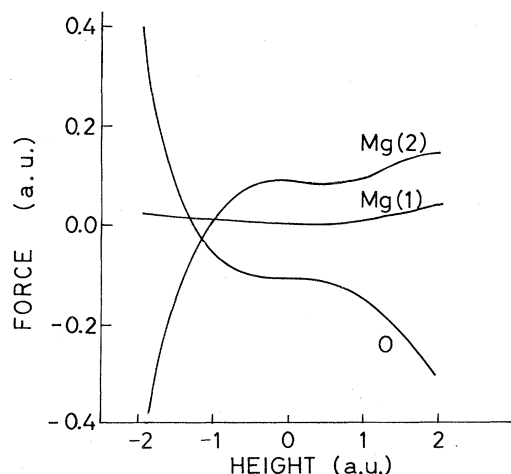


FIG. 9. Forces acting on the O, the first-layer Mg(1), and the second-layer Mg(2) atoms of the O/Mg<sub>4</sub> cluster as functions of the oxygen height. The positive (negative) force is defined to be in the direction out of (into) the surface. The positive (negative) height corresponds to the position above (below) the surface.

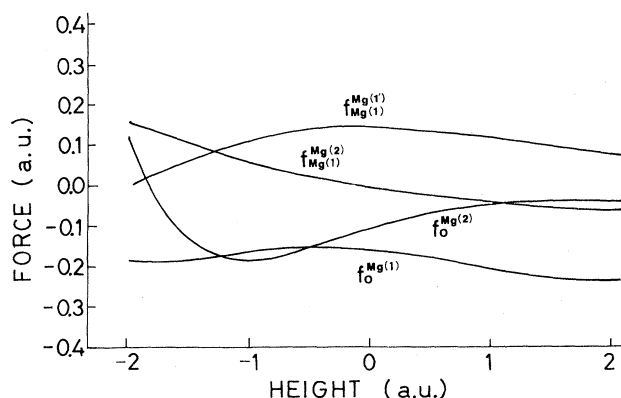


FIG. 10. Effective pair forces among the O, the first-layer Mg(1), and the second-layer Mg(2) atoms as functions of oxygen height. The positive force is defined to be in the direction of the pair bond, i.e., repulsive. The positive (negative) height corresponds to the position above (below) the surface.

## V. DISCUSSION

According to the calculated force in the preceding section, the activation energy for oxygen penetration into the surface is about 1 eV on the Al surface and 0 eV for the Mg surface. This is due to the difference in the properties of the surface bonding. The difference in the electronic structures of the Al and Mg surfaces comes from the  $3e$  level which can be occupied or unoccupied. The  $3e$  state consists mainly of the  $3p$  state of Al and Mg. The wave functions of the doubly degenerate  $3e$  orbitals are given as

$$\psi_{3e_1} = C_1 \left[ \frac{1}{\sqrt{2}} \chi_{2z} - \frac{1}{\sqrt{2}} \chi_{3z} \right] + C \left[ \frac{1}{\sqrt{2}} \chi_{2x} - \frac{1}{\sqrt{2}} \chi_{3x} \right] + \dots$$

and

$$\psi_{3e_2} = C_1 \left[ \frac{2}{\sqrt{6}} \chi_{1z} - \frac{1}{\sqrt{6}} \chi_{2z} - \frac{1}{\sqrt{6}} \chi_{3z} \right] + C_2 \left[ \frac{2}{\sqrt{6}} \chi_{1x} - \frac{1}{\sqrt{6}} \chi_{2x} - \frac{1}{\sqrt{6}} \chi_{3x} \right] + \dots,$$

where  $\chi_{\mu z}$  and  $\chi_{\mu x}$  are the atomic  $3p$  orbitals of the first-layer  $\mu$ th Al in the direction perpendicular and parallel to the surface, respectively, as shown in Fig. 11. The coefficients  $C_1$  and  $C_2$  depend on oxygen height. The ratio of the  $C_1$  to  $C_2$  determines the direction of the  $3p$ -orbital lobe, as shown in Fig. 11. If  $C_1 = 0.0$  and  $C_2 = 1.0$ , one has  $\theta = 0.0^\circ$ , and if  $C_1 = -1.0$  and  $C_2 = 0.0$ , one has  $\theta = \pi/2$  (in deg). The direction of the  $3p$ -orbital lobe from the surface is shown in Fig. 11 as a function of oxygen height.

When the oxygen is located at  $+\infty$ , the lobe of the Al(1)  $3p$  orbital is directed to the center of the tetrahedron Al(1)Al(1')Al(1'')Al(2), as shown in Fig. 4, giving  $\theta = 20^\circ$ . Thus the  $3p$  electron contributes equally to three bonds, Al(1)–Al(1'), Al(1)–Al(1''), and Al(1)–Al(2).

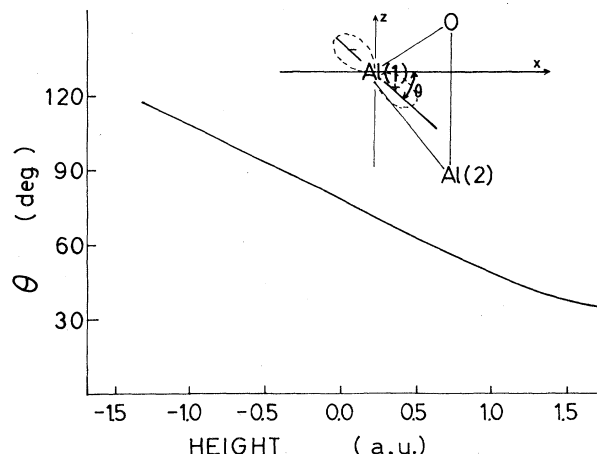


FIG. 11. Angle direction of the  $3p$ -orbital lobe of the Al(1) in the highest occupied  $3e$  orbital.

The direction of the  $3p$ -orbital lobe changes when oxygen approaches the surface, because the bonding of the Al  $3p$  orbital with the O  $2p$  orbital has antibonding character. The approach of oxygen tends to break the bond between the surface atom Al(1) and the inside atom Al(2), and makes a new bond between the oxygen and surface Al(1) atoms. The bonding between the Mg atoms is mainly due to  $3s$  electrons. Therefore, the bonding property of the Mg atoms is not directional compared to that of the Al atoms. The bonding of the Mg surface atoms is more insensitive to the approach of oxygen to the surface than is the Al surface bonding: Oxygen on the Mg surface bonds with the Mg surface atoms without breaking the bond between the Mg atoms.

The pair forces between chemisorbed oxygen and the metal atoms determine the order of magnitude of the activation barrier for oxygen penetration into the surface. The interaction of oxygen with the first-layer metal atoms is similar to that of the corresponding diatomic molecule. However, the interaction with the second-layer atoms is more complicated. It is induced by the indirect interaction through the first-layer atoms as well as the direct interaction with the second-layer atom. The direct interaction seems to be similar to that of the diatomic molecule. The indirect interaction depends upon the interaction between the first- and second-layer atoms, as the oxygen orbitals are spread over the first-layer atoms. The order of the indirect interaction may be directly proportional to the product of the direct interaction between the Al(1) and the Al(2) atoms and the mixing coefficients between the wave functions of the oxygen atom and the first-layer Al(1) atom. Since the pair force between the Al(1) and Al(2) atoms is more repulsive than that between the Mg(1) and Mg(2) atoms, the extended oxygen orbitals on the Al surface interact repulsively with the underlayer Al metals.

The virials are equal to zero if all of the atoms in the cluster are in their equilibrium positions. In our model cluster, however, the metal atoms are assumed to be fixed at the bulk positions, so that the virials are nonvanishing. The full optimization of the geometry is useless in the cluster approximation because the atoms of the cluster



surface are bound to surrounding metal atoms. The pressure of the cluster against the surrounding atoms is estimated from the virials. The pressure of the cluster at the Al surface is always higher than that of the Mg surface when the oxygen atom approaches the surface. This means that the oxygen atom is more easily chemisorbed on the Mg surface than on the Al surface.

In this paper we have learned a great deal about the oxidation mechanism of the Al and Mg surfaces. From this we can make the following speculation on the oxidation of the silicon and sodium surfaces. In the case of Si, the Si-Si bond is known to be due to the  $3p$  orbitals of the Si atoms. Therefore, oxygen on the silicon surface would break the Si-Si bonds, and would be chemisorbed on the surface without being absorbed below the surface as in the case of Al. On the other hand, the Na-Na bond is known to be due to the  $3s$  orbitals of the Na atom. Therefore, the oxygen atom would be absorbed below the surface without an activation energy, because the oxygen on the surface would not break the bond between the Na atoms as in the case of Mg.

## VI. CONCLUDING REMARKS

We have formulated the force and the virial in the LCAO and LCPW approximations. We have seen the importance of the correction terms in the LCAO approximation; the correction term in the force formula is indeed very large. The correction term in the virial formula is smaller than that in the force formula, but it is not negligible for the quantitative analysis of the system.

The force and virial analysis has elucidated the chemisorption process of oxygen on Al(111) and Mg(0001). The stresses on the Al or Mg atoms surrounding an absorbed oxygen atom have been determined directly. The different behavior of oxygen on the Mg and Al surfaces have been understood by seeing the difference in the metal-metal bond. The bond between the Al atoms is directional, while the bond between the Mg atoms is spherical. The strong bond between the surface atoms in-

duces the absorption activation energy. Although the size of our cluster model is small, we have already obtained a reasonable bond distance for oxygen and aluminum on the surface.

We are now applying the present force and virial analysis to the study of the equilibrium configuration of the surface atoms, the absorbed atoms, and the atoms around surface defects. We are also studying the vibrational modes of one-dimensional infinite polymers and dissociative chemisorption with this method. The results of these calculations are reported elsewhere.<sup>34,35</sup>

## ACKNOWLEDGMENTS

I gratefully acknowledge Professor S. Sugano for a critical reading of this manuscript and for helpful comments. I thank Professor K. Morokuma for his continued encouragement of this work and for helpful discussions. Numerical calculations were carried out at the Computer Center of the Institute for Molecular Science on a HITAC M-200 computer.

## APPENDIX A

The Eqs. (26), (28), and (29) for the pair forces are derived herein. The force acting on the nuclear charge depends on the atomic orbitals used. We decompose the total force  $\vec{F}_\mu$  of Eq. (19) into the forces acting on the nuclear charge and on the surrounding electron density  $\rho_\mu(\vec{r})$ , which is defined by Eq. (22).

The derivative in the correction term  $\vec{F}_{\mu 2}$  is written [by using Eq. (23)] as

$$\frac{\partial \psi_i}{\partial \vec{R}_\mu} = - \sum_\mu \frac{\partial \psi_{i\mu}}{\partial \vec{r}}. \quad (\text{A1})$$

The correction term is expressed as the sum of the forces acting on the electronic charge and others as

$$\vec{F}_{\mu 2} = - \int \rho_\mu(\vec{r}) \vec{E}(\vec{r}) d\vec{v} + \frac{1}{2} \left[ \sum_i^{\text{occ}} \int d\vec{v} \left( \frac{\partial \psi_{i\mu}^*}{\partial \vec{r}} (h - \epsilon_i) \psi_i - \psi_{i\mu} (h - \epsilon_i) \frac{\partial \psi_i^*}{\partial \vec{r}} \right) + \text{c.c.} \right] + \int \frac{d\rho_\mu(\vec{r})}{d\vec{r}} V_{xc}(\vec{r}) d\vec{v}. \quad (\text{A2})$$

Here, partial integration of Eq. (21) and a little algebraic manipulation are performed. In Eq. (A2) the electric field  $E(r)$  is written as

$$\vec{E}(\vec{r}) = \sum_\tau \vec{E}_\tau(\vec{r}), \quad (\text{A3})$$

where the  $\vec{E}_\tau(\vec{r})$  are given by Eq. (27). The last term of Eq. (A2) may be written, by using partial integration, as

$$\int \frac{d\rho_\mu}{d\vec{r}} V_{xc}(\vec{r}) d\vec{v} = - \int \rho_\mu \frac{dV_{xc}(\vec{r})}{d\vec{r}} d\vec{v} = \frac{1}{4} \int \left( \frac{d\rho_\mu}{d\vec{r}} \rho - \frac{d\rho}{d\vec{r}} \rho_\mu \right) V_{xc}(\vec{r}) \rho^{-1}(\vec{r}) d\vec{v}. \quad (\text{A4})$$

The electrostatic pair force is obtained from the term involving the electric field  $\vec{E}_\tau(\vec{r})$  due to the  $\tau$ th atom. The deformed-charge pair force and the exchange pair force are obtained from the other terms.

## APPENDIX B

Here we prove the virial formula in Eq. (34) by using the force formula in Eq. (19). Upon using Eq. (19) and the relations  $\vec{r}_\mu = \vec{r} - \vec{R}_\mu$  and  $\vec{R}_{\mu\nu} = \vec{R}_\mu - \vec{R}_\nu$ , the virial can be written as

$$\sum_{\mu} \vec{R}_{\mu} \cdot \vec{F}_{\mu} = \frac{1}{2} \sum_{\mu, \nu}' \frac{Z_{\mu} Z_{\nu}}{R_{\mu\nu}} + \sum_{\mu} Z_{\mu} \int \rho(\vec{r}) \frac{\vec{R}_{\mu} \cdot \vec{r}_{\mu}}{r_{\mu}^3} dv - \left[ \sum_{\mu} \sum_i \int \vec{r}_{\mu} \cdot \frac{\partial \psi_{i\mu}^*}{\partial \vec{r}} (h - \epsilon_i) \psi_i dv + \text{c.c.} \right] + \left[ \sum_i^{\text{occ}} \int \vec{r} \cdot \frac{\partial \psi_i^*}{\partial \vec{r}} (h - \epsilon_i) \psi_i dv + \text{c.c.} \right]. \quad (\text{B1})$$

The last term on the right-hand side of (B1) may be partially integrated and transformed by the use of the relation  $\vec{r}h = h\vec{r} + \vec{\nabla}$  into the expression

$$\sum_i^{\text{occ}} \left[ \vec{r} \cdot \frac{\partial \psi_i}{\partial \vec{r}}, (h - \epsilon_i) \psi_i \right] + \text{c.c.} = - \sum_i^{\text{occ}} \left[ \psi_i, \vec{r} \cdot \frac{\partial h}{\partial \vec{r}} \psi_i \right] + 2E_{\text{kin}}. \quad (\text{B2})$$

Then the virial can be written as

$$\sum_{\mu} \vec{R}_{\mu} \cdot \vec{F}_{\mu} = 2E_{\text{kin}} - \left[ \sum_{\mu} \sum_i^{\text{occ}} \int \vec{r}_{\mu} \cdot \frac{\partial \psi_{i\mu}^*}{\partial \vec{r}} (h - \epsilon_i) \psi_i dv + \text{c.c.} \right] + \frac{1}{2} \sum_{\mu, \nu}' \frac{Z_{\mu} Z_{\nu}}{R_{\mu\nu}} + \sum_{\mu} Z_{\mu} \int \rho(\vec{r}) \frac{\vec{R}_{\mu} \cdot \vec{r}_{\mu}}{r_{\mu}^3} dv - \sum_i^{\text{occ}} \left[ \psi_i, \vec{r} \cdot \frac{\partial h}{\partial \vec{r}} \psi_i \right]. \quad (\text{B3})$$

In the last term of the above equation, the operator  $\vec{r} \cdot (\partial h / \partial \vec{r})$  can be expressed as

$$\vec{r} \cdot \frac{\partial h}{\partial \vec{r}} = \sum_{\mu} \frac{Z_{\mu}}{r_{\mu}} + \sum_{\mu} \frac{Z_{\mu} \vec{R}_{\mu} \cdot \vec{r}_{\mu}}{r_{\mu}^3} - \int \rho(\vec{r}') \frac{\vec{r} \cdot (\vec{r} - \vec{r}')}{|\vec{r} - \vec{r}'|^3} dv'. \quad (\text{B4})$$

Then, inserting Eq. (B4) into (B3), we obtain the virial formula

$$\sum_{\mu} \vec{R}_{\mu} \cdot \vec{F}_{\mu} = 2E_{\text{kin}} + \vec{V} - \left[ \sum_{\mu} \sum_i^{\text{occ}} \int \vec{r}_{\mu} \cdot \frac{\partial \psi_{i\mu}^*}{\partial \vec{r}} (h - \epsilon_i) \psi_i dv + \text{c.c.} \right], \quad (\text{B5})$$

where the kinetic energy  $E_{\text{kin}}$  and the potential energy  $V$  are given as

$$E_{\text{kin}} = \sum_i^{\text{occ}} \left[ \psi_i, -\frac{\vec{\nabla}^2}{2} \psi_i \right] \quad (\text{B6})$$

and

$$V = \frac{1}{2} \sum_{\mu, \nu}' \frac{Z_{\mu} Z_{\nu}}{R_{\mu\nu}} - \sum_{\mu} Z_{\mu} \int \frac{\rho(\vec{r})}{r_{\mu}} dv + \frac{1}{2} \iint \frac{\rho(\vec{r}) \rho(\vec{r}')}{|\vec{r} - \vec{r}'|} dv dv' + E_{\text{xc}}, \quad (\text{B7})$$

respectively.

<sup>1</sup>J. C. Slater, J. Chem. Phys. **57**, 2389 (1972).

<sup>2</sup>H. C. White, Phys. Rev. **112**, 1092 (1958).

<sup>3</sup>N. D. Lang and A. R. Williams, Phys. Rev. Lett. **34**, 531 (1975).

<sup>4</sup>J. Koller, M. Zaucer, and A. Azman, Z. Naturforsch **31a**, 1022 (1976).

<sup>5</sup>D. A. Liberman, Phys. Rev. **3**, 2081 (1971).

<sup>6</sup>J. F. Janak, Phys. Rev. B **9**, 3985 (1974).

<sup>7</sup>F. W. Averill and G. Painter, Phys. Rev. B **24**, 6795 (1981).

<sup>8</sup>J. Ihm, A. Zunger, and M. L. Cohen, J. Phys. C **12**, 4409 (1979).

<sup>9</sup>J. Ihm, M. T. Yin, and M. L. Cohen, Solid State Commun. **37**, 491 (1981).

<sup>10</sup>K. Kunc and R. M. Martin, Phys. Rev. Lett. **48**, 406 (1982).

<sup>11</sup>J. Harris, R. O. Jones, and J. E. Müller, J. Chem. Phys. **75**, 3904 (1981).

<sup>12</sup>P. Pulay, in *Modern Theoretical Chemistry*, edited by H. F. Schaefer III (Plenum, New York, 1977), Vol. 4, p. 153; A. Komornicki, K. Ishida, K. Morokuma, R. Ditchfield, and M.

Conrad, Chem. Phys. Lett. **45**, 595 (1977).

<sup>13</sup>C. Satoko, Chem. Phys. Lett. **83**, 111 (1981). Recently, the same formula with Eq. (9) in the above paper was obtained independently by P. Bendt and A. Zunger [Phys. Rev. Lett. **50**, 1684 (1983)].

<sup>14</sup>J. C. Slater, *The Self-Consistent Field for Molecules and Solids* (McGraw-Hill, New York, 1974), p. 290.

<sup>15</sup>A. H. Strout, *Approximate Calculations of Multiple Integrals* (Prentice-Hall, Englewood Cliffs, New Jersey, 1971).

<sup>16</sup>R. Z. Bachrach, G. V. Hansen, and R. S. Bauer, Surf. Sci. **109**, L560 (1981).

<sup>17</sup>B. Kasemo, E. Tornqvist, J. K. Norskov, and B. I. Lundqvist, Surf. Sci. **89**, 554 (1979).

<sup>18</sup>G. C. Allen, P. M. Tucker, B. E. Hayden, and D. F. Klemperer, Surf. Sci. **102**, 207 (1981).

<sup>19</sup>C. W. B. Martinson and S. A. Flodstrom, Solid State Commun. **30**, 671 (1979).

<sup>20</sup>H. Namba, J. Darville, and J. M. Gilles, Surf. Sci. **108**, 446 (1979).

- <sup>21</sup>K. Shinjo, S. Sugano, and T. Sasada, *Phys. Rev. B* **28**, 5570 (1983).
- <sup>22</sup>K. P. Huber and G. Herzberg, *Constant of Diatomic Molecules* (Van Nostrand Reinhold, New York, 1979).
- <sup>23</sup>C. W. B. Martinson and S. A. Flodstrom, *Solid State Commun.* **30**, 671 (1979).
- <sup>24</sup>M. R. Martin and G. A. Somorjai, *Phys. Rev. B* **7**, 3607 (1973).
- <sup>25</sup>A. Bianconi and R. Z. Bachrach, *Phys. Rev. Lett.* **42**, 104 (1979).
- <sup>26</sup>K. Y. Yu, J. N. Miller, P. Chye, W. E. Spicer, N. D. Lang, and A. R. Williams, *Phys. Rev. B* **14**, 1446 (1976).
- <sup>27</sup>S. A. Flodstrom, C. W. B. Martinson, R. Z. Bachrach, S. B. M. Hagstrom, and R. S. Bauer, *Phys. Rev. Lett.* **40**, 907 (1978).
- <sup>28</sup>D. R. Salahub, M. Roche, and R. P. Messmer, *Phys. Rev. B* **18**, 6495 (1978).
- <sup>29</sup>D. Wang, A. J. Freeman, and H. Krakauer, *Phys. Rev. B* **24**, 3104 (1981).
- <sup>30</sup>L. I. Johansson and J. Stohr, *Phys. Rev. Lett.* **43**, 1882 (1979).
- <sup>31</sup>C. W. B. Martinson, S. A. Flodstrom, J. Rundgren, and P. Westrin, *Surf. Sci.* **89**, 102 (1979).
- <sup>32</sup>R. W. G. Wyckoff, *Crystal Structure*, 2nd ed. (Interscience, New York, 1963).
- <sup>33</sup>J. C. Fuggle, *Surf. Sci.* **69**, 581 (1977).
- <sup>34</sup>C. Satoko and M. Tsukada, *Surf. Sci.* **134**, 1 (1983).
- <sup>35</sup>H. Teramae, T. Yamabe, C. Satoko, and A. Imamura, *Chem. Phys. Lett.* **101**, 149 (1983).